2024 European Control Conference (ECC)
June 25-28, 2024. Stockholm, Sweden

Reliability-oriented Current Sharing and Voltage Balancing in DC Microgrids: An LPV-based Approach

Mahdieh S. Sadabadi

Abstract— **This paper proposes a reliability-aware secondary control scheme for power-electronics-dominated DC microgrids with an additional goal of enhancing the microgrid's reliability. The main goal of the paper is to enforce components' reliability, modeled as time-varying parameters, into a reliability-oriented power sharing and voltage balancing. To this end, a DC microgrid under the degradation process of power converters' parameters is modeled by a linear parameter varying (LPV) system. By virtue of this novel description and leveraging tools from stability analysis and control synthesis of LPV systems, as well as insights from the physics of microgrids, the paper develops a novel reliability-oriented distributed secondary control scheme. The proposed scheme does not rely on the topology of microgrids nor the parameters of power lines; it guarantees stability, voltage balancing, and current sharing while taking the reliability aspects and stability constraints into the control design process. Simulation results verify the performance and effectiveness of the proposed secondary control approach.**

I. Introduction

Microgrids are examples of cyber-physical systems that include electrical components (physical layer) as well as sensing, control, computing, and communication elements (cyber layer) [1]. Such systems are subject to several sources of stress in their cyber layer, such as cyberattacks [2]. Besides the cyber stresses, the physical layer of microgrids is exposed to physical stresses, e.g., component aging, fatigue, and degradation [3]. Due to the tight interaction between the cyber and physical layers in microgrids, local stresses in any part of these layers can propagate throughout the microgrid and threaten its reliable and normal operation. Due to the relatively low system inertia of microgrids, cyber or physical stresses might result in large disturbances, deteriorate microgrids' normal functionalities, threaten their stability, and also cause physical damage to loads and power electronics devices.

Conventional control systems for microgrids consider robustness to modeling uncertainties including load variation and plug-and-play operation of converter-based resources, in their design. However, they are not intrinsically robust to cyber and physical stresses in power-electronics-rich microgrids. Given that the main goal of microgrids is to enhance the reliability and resilience of energy supply, it is crucial to enhance microgrids' reliability and their resilience to cyber-physical stresses.

The main focus of this paper is on enhancing the reliability of microgrids against physical stresses, particularly on the reliability of power electronics converters. Capacitors and semiconductor devices that are the most failure-prone components in power electronics converters are exposed to aging and wear-out failures, as a result of intermittent operating and environmental conditions (e.g., power loading, ambient temperature, and humidity) [4]. Such failures challenge the reliability of power-electronics-interfaced microgrids, as the failures might propagate into the whole system (cascading failure) and lead to serious performance degradation at the system level and unscheduled costly maintenance or result in overall system failure. The investigation of the reliability of PV systems in [5] reveals that the most frequently failed subsystem is power converter converters.

The existing research on the reliability of power-electronics-dominated microgrids can be classified into two groups, converter or component-level approaches, see the survey papers in [6], and system-level approaches, e.g., [7]. The existing methods on the converter or component-level reliability mostly rely on condition monitoring and online parameter identification (dc-link capacitors, equivalent series resistance (ESR) of transistors, etc.), e.g., [8]–[10]. While the research in the reliability of power electronics converters (component level) is substantial, the reliability at the system level (microgrid level) has not been fully investigated. The existing methods for system-level reliability in microgrids mostly focus on reliability-oriented power sharing. The main idea is to share load power among power converters such that those with higher damage contribute less and healthier converters contribute more in the power-sharing scheme [7]. This is done by adjusting the droop coefficients in a power-sharing scheme. The reliability-oriented power-sharing enforces the redistribution of power among converters to prolong the lifetime of the entire system. However, adjusting droop gains based on the health of power converters in this approach is open-loop and does not consider the stability constraints in the design of droop gains. To address this issue, in [11] a framework of stability-constrained reliability-oriented droop control is proposed. However, this approach suffers from the lack of rigorous stability analysis. To the best of our knowledge, concise stability certificates in reliability-oriented control of microgrids is missing in the literature.

Inspired by the existing gaps and drawbacks of system-level approaches for enhancing reliability in microgrids, this paper aims to develop a reliability-aware secondary control solution that enforces reliability measures in the control design phase. To this end, a DC microgrid under the degradation process of power converters' parameters is described by a linear parameter varying (LPV) system [12], a modeling framework suited for capturing the time-varying

M. S. Sadabadi is with the Department of Electrical and Electronic Engineering, University of Manchester, Manchester, United Kingdom, mahdieh.sadabadi@manchester.ac.uk.

changes in the parameters of a dynamical system. Under this novel description and leveraging tools from stability analysis and control synthesis of LPV systems, as well as insights from the physics of microgrids, the paper develops a novel reliability-aware distributed secondary control scheme. Such a reliability-by-design control approach presents a clear advantage over conventional secondary control mechanisms in microgrids, where stability and performance criteria are only considered. The efficiency of the proposed control strategy is evaluated by simulation case studies.

Notation: The notations used in this paper are standard. In particular, matrix $\mathbf{I}_n$ is an $n \times n$ identity matrix, $\mathbf{0}_{n\times m}$ is an $n \times m$ matrix of zeros, and $\mathbf{1}_n$ is an n-dimensional vector of all ones. The symbols A^T, $rank(A)$, $ker(A)$, $det(A)$, $trace(A)$, $\star$, and $\mathrm{diag}(a_1, \ldots, a_n)$ respectively denote the transpose, the rank, the kernel (null space), the determinant, the trace of A, the symmetric block in a symmetric matrix, and a diagonal matrix whose diagonal elements are a_i. For an $n \times n$ diagonal matrix X, $vec(X)$ is an $n \times 1$ vector whose elements are diagonal entities of X. For symmetric matrices, $P \succ 0$ ($P \prec 0$) and $P \succeq 0$ ($P \preceq 0$) respectively indicate the positive-definiteness (negative-definiteness) and the positive semi-definiteness (negative semi-definiteness).

II. Modeling of DC Microgrids

Consider a Kron-reduced DC microgrid composed of n converter-interfaced distributed generation (DG) units that are interconnected by m resistive–inductive distribution lines. Using the circuit theory, the converter-interfaced DG unit i is mathematically modeled as follows:

$$\begin{aligned} C_{t_i}\dot{V}_i(t) &= I_{t_i}(t) - Y_i V_i(t) - \sum_{k=1}^{m} \mathbb{B}_{e,ik} I_k(t), \\ L_{t_i}\dot{I}_{t_i}(t) &= -V_i(t) - R_{t_i} I_{t_i}(t) + V_{dc,i} d_i(t), \end{aligned} \tag{1}$$

for $i \in \{1, \ldots, n\}$, where $V_i(t) \in \mathbb{R}$, $I_{t_i}(t) \in \mathbb{R}$, $d_i(t) \in \mathbb{R}$ are the voltage at the Point of Common Coupling (PCC) i, the filter current, and the duty cycle of the DC-DC converter i, respectively. In the dynamic equations in (1), L_{t_i}, R_{t_i}, C_{t_i}, Y_i, and $V_{dc,i}$ represent the filter inductance of the converter i, the ESR of the inductance L_{t_i}, a shunt capacitance, load conductance and the DC voltage at the input side of the converter i, respectively. The dynamics of the line k are described as follows:

$$L_k \dot{I}_k(t) = -R_k I_k(t) + \sum_{j=1}^{n} \mathbb{B}_{e,jk} V_j(t), \tag{2}$$

for $k \in \{1, \ldots, m\}$ where $I_k(t)$, R_k, and L_k are the line current, resistance, and inductance, respectively. The term $\mathbb{B}_{e,ik}$ is formulated as follows [13]:

$$\mathbb{B}_{e,jk} = \begin{cases} 1 & \text{if line } k \text{ leaves DG } j, \\ -1 & \text{if line } k \text{ enters DG } j, \\ 0 & \text{otherwise.} \end{cases} \tag{3}$$

Given the dynamics of DG units in (1) and lines in (2) and denoting $V = [V_1, \ldots, V_n]^T$, $I_t = [I_{t_1}, \ldots, I_{t_n}]^T$, $I = [I_1, \ldots, I_m]^T$, and $d = [d_1, \ldots, d_n]^T$, the physical layer of DC microgrids can be described in a vector form as follows:

$$\begin{aligned} C_t \dot{V}(t) &= I_t(t) - YV(t) - \mathbb{B}_e I_k(t), \\ L_t \dot{I}_t(t) &= -V(t) - R_t I_t(t) + V_{dc} d(t), \\ L\dot{I}(t) &= -RI(t) + \mathbb{B}_e^T V(t), \end{aligned} \tag{4}$$

where $C_t = \mathrm{diag}(C_{t_1}, \ldots, C_{t_n})$, $L_t = \mathrm{diag}(L_{t_1}, \ldots, L_{t_n})$, $R_t = \mathrm{diag}(R_{t_1}, \ldots, R_{t_n})$, $Y = \mathrm{diag}(Y_1, \ldots, Y_n)$, $V_{dc} = \mathrm{diag}(V_{dc,1}, \ldots, V_{dc,n})$, $L = \mathrm{diag}(L_1, \ldots, L_m)$, $R = \mathrm{diag}(R_1, \ldots, R_m)$, and $\mathbb{B}_e$ is the incidence matrix of the graph representing the topology of the microgrid.

A. An LPV-based Modeling Framework of DC Microgrids

Power electronics converters are prone to degradation and failure due to several reasons including aging and operational conditions, e.g., operating under electrical stress and variable power sources in power conversion applications, such as electric vehicles and renewable energy resources [14]. In these applications, some key components such as electrolytic capacitors degrade over time due to the evaporation of the electrolyte [14]. In general, DC link capacitors are one of the most vulnerable components in power electronics circuits [15]. In this section, an LPV framework is proposed for power-electronics-based DC microgrids to model the time-varying characteristics of their key components such as capacitances, inductances, and their ESRs. To this end, C_{t_i}, L_{t_i}, and R_{t_i} in (1) are considered as time-varying parameters. The microgrid dynamics in (1) can be embedded into a linear parameter-varying representation as follows:

$$\begin{aligned} \dot{x}(t) &= A(\rho)x(t) + B(\rho)u(t), \\ y(t) &= Cx(t), \end{aligned} \tag{5}$$

where $x(t) = [V^T(t)\ I_t^T(t)\ I^T(t)]^T$ is the state, $u(t) = d(t)$ is the input, and $y(t) = [V^T(t)\ I_t^T(t)]^T$ is the output. The state space matrices in (5) are defined as follows:

$$A(\rho) = \begin{bmatrix} -C_t^{-1}(t)Y & C_t^{-1}(t) & -C_t^{-1}(t)\mathbb{B}_e \\ -L_t^{-1}(t) & -L_t^{-1}(t)R_t(t) & \mathbf{0}_{n\times m} \\ L^{-1}\mathbb{B}_e^T & \mathbf{0}_{m\times n} & -L^{-1}R \end{bmatrix},$$
$$B(\rho) = \begin{bmatrix} \mathbf{0}_{n\times n} \\ L_t^{-1}(t)V_{dc} \\ \mathbf{0}_{m\times n} \end{bmatrix},\ C = \begin{bmatrix} \mathbf{I}_n & \mathbf{0}_{n\times n} & \mathbf{0}_{n\times m} \\ \mathbf{0}_{n\times n} & \mathbf{I}_n & \mathbf{0}_{n\times m} \end{bmatrix}. \tag{6}$$

In the LPV representation in (5), the scheduling parameters are $\rho = [vec(C_t(t))^T\ vec(L_t(t))^T\ vec(R_t(t))^T]^T \in \mathbb{R}^{3n\times 1}$.

Due to the degradation process and wear-out, the value of capacitors and inductors decreases while the value of their ESR increases. The recent studies show that in aluminum electrolytic capacitors, the capacitance reduction is up to 20%, whereas in film capacitors, the reduction values are up to 2% to 5% [16]. Hence, the scheduling variable ρ is assumed to belong to a polyhedron Φ defined by

$$\begin{aligned} C_{t_i,min} \le C_{t_i}(t) \le C_{t_i,nom}, \\ L_{t_i,min} \le L_{t_i}(t) \le L_{t_i,nom}, \\ R_{t_i,nom} \le R_{t_i}(t) \le R_{t_i,max}, \end{aligned} \tag{7}$$

where the index "nom", "min", and "max" respectively define the nominal, minimum, and maximum values. In addition, the rate of variation of these parameters ($\dot{\rho}$) is bounded and satisfies the following constraints [16]:

$$\frac{d}{dt}C_{t_i}(t) \leq 0,\ \frac{d}{dt}L_{t_i}(t) \leq 0,\ \frac{d}{dt}R_{t_i}(t) \geq 0. \tag{8}$$

for $i = 1, \ldots, n$.

III. Reliability-oriented Control

A. Current Sharing and Voltage Balancing Objectives

Current sharing is one of the objectives in the secondary control of DC microgrids where the aim is to proportionally share total load demands amongst DG units at the steady-state according to the rated currents of DG units, i.e.,

$$\lim_{t\to\infty}\left(\frac{I_{t_i}(t)}{I_i^{rated}} - \frac{I_{t_j}(t)}{I_j^{rated}}\right) = 0, \quad i,j \in \{1,\ldots,n\},\ i \neq j, \tag{9}$$

where $I_{t_i}(t)$, $I_{t_j}(t)$, I_i^{rated}, and I_j^{rated} are the current of the converter i and converter j, the rated current of converter i, and the rated current of converter j, respectively.

The second secondary control objective in DC microgrids is the voltage balancing defined as follows:

$$\lim_{t\to\infty}\frac{1}{n}\sum_{i=1}^{n} I_i^{rated}(V_i(t) - V^*) = 0. \tag{10}$$

where V^* is a given nominal voltage reference of microgrids.

The main objective of this paper is to develop a secondary control scheme to ensure the current sharing and voltage balancing objectives in (9) and (10) while taking the reliability aspects into the design process.

B. Proposed Primary Control Scheme

The proposed primary control scheme is based on a PI controller whose structure is given as follows:

$$\begin{aligned} u_i(t) &= K_{P_i}V_i(t) + K_{I_i}v_i(t) + K_i w_i(t),\\ \dot{v}_i &= -V_i(t) + V^* - w_i(t), \end{aligned} \tag{11}$$

where $u_i(t) = V_{dc,i}d_i(t)$, K_{P_i} is the proportional gain, K_{I_i} is the integral gain, K_i is a control gain, and $w_i(t)$ is the correction term sent by a secondary control layer (see Subsection III-C). Theorem 1 in Subsection III-D discusses the design of the control parameters K_{P_i}, K_{P_i}, and K_i for guaranteeing closed-loop stability.

Note that when the secondary control scheme is inactive, the correction term $w_i = 0$ in (11). In this case, exact voltage regulation can be achieved via the PI-based primary controller in (11). However, the current sharing objective in (9) is no longer ensured. The secondary control layer is designed to achieve both current sharing and voltage balancing objectives formulated in (9) and (10). In the following, a consensus-based reliability-oriented secondary control scheme is proposed.

C. Proposed Reliability-oriented Secondary Control Scheme

To achieve the current sharing objective in (9), a distributed consensus-based integral secondary control scheme is required. To this end, a control state $x_i^c(t)$ is considered whose aim is to ensure the current sharing among DG units by sharing or coordination through distributed computations. The dynamics of $x_i^c(t)$ are described as follows:

$$\dot{x}_i^c(t) = \alpha\sum_{i=1,i\neq j}^{n}\eta_{ij}\left(\frac{I_{t_i}(t)}{I_i^{rated}} - \frac{I_{t_j}(t)}{I_j^{rated}}\right), \tag{12}$$

where $\alpha \in \mathbb{R}_{>0}$ is an integral gain and $\eta_{ij} \in \mathbb{R}_{\geq 0}$ is a communication weight between DG i and DG j, determined based on the communication topology in the cyber layer of microgrids. The secondary controller sends the following correction term to the PI-based primary controller in (11):

$$w_i(t) = \frac{1}{I_i^{rated}}\sum_{i=1,i\neq j}^{n}\eta_{ij}(x_{c_i}(t) - x_{c_j}(t)), \tag{13}$$

Assumption 1. *The undirected graph in the proposed secondary control scheme is assumed to be connected.*

D. Equilibrium (Steady-state) Analysis

Denoting $x^c(t) = [x_1^c, \ldots, x_n^c]^T$, $w(t) = [w_1, \ldots, w_n]^T$, and $v(t) = [v_1, \ldots, v_n]^T$, the proposed cyber-physical DC microgrids can be described in a vector form as follows:

$$\begin{aligned} \dot{x}_{cl}(t) &= A_{cl}(\rho)x_{cl}(t) + B_{cl}(\rho)V^*,\\ y(t) &= C_{cl}x_{cl}(t), \end{aligned} \tag{14}$$

where $x_{cl}(t) = [x^T(t)\ x_c^T(t)]^T$ is the closed-loop state vector, $x_c(t) = [v^T(t)\ x^{cT}(t)]^T$ is the augmented primary-secondary control state vector and state space matrices are given in (15). In (15), $\mathcal{L}_c$ is the Laplacian matrix associated with the communication topology in the secondary control layer, $W = \text{diag}(\frac{1}{I_1^{rated}}, \ldots, \frac{1}{I_n^{rated}})$, $K = \text{diag}(K_1, \ldots, K_n)$, $K_P = \text{diag}(K_{P_1}, \ldots, K_{P_n})$, and $K_I = \text{diag}(K_{I_1}, \ldots, K_{I_n})$.

Remark 1. *Under Assumption 1, it can be shown that the control state trajectories $x_c(t)$ in* (12) *satisfy the following condition:*

$$\mathbf{1}_n^T x_c(t) = \mathbf{1}_n^T x_c(0),\ \forall t > 0. \tag{16}$$

The above equation is a conservation law for the dynamics of (12)*.*

For the closed-loop system in (14), the set of equilibrium points is defined as follows:

$$\mathcal{E} = \{\bar{x}_{cl} \in \mathbb{R}^{4n+m} \mid A_{cl}(\rho)\bar{x}_{cl} + B_{cl}(\rho)V^* = \mathbf{0}_{(4n+m)\times 1}\}. \tag{17}$$

According to (14), the equilibrium point $\bar{x}_{cl} = [\bar{V}^T\ \bar{I}_t^T\ \bar{I}^T\ \bar{v}^T\ \bar{x}^{c^T}]^T$ of the closed-loop dynamics in (14)

$$A_{cl}(\rho)=\begin{bmatrix} -C_t^{-1}(t)Y & C_t^{-1}(t) & -C_t^{-1}(t)\mathbb{B}_e & \mathbf{0}_{n\times n} & \mathbf{0}_{n\times n} \\ L_t^{-1}(t)(-\mathbf{I}_n+K_P) & -L_t^{-1}(t)R_t(t) & \mathbf{0}_{n\times m} & L_t^{-1}(t)K_I & L_t^{-1}(t)KW\mathcal{L}_c \\ L^{-1}\mathbb{B}_e^T & \mathbf{0}_{m\times n} & -L^{-1}R & \mathbf{0}_{m\times n} & \mathbf{0}_{m\times n} \\ -\mathbf{I}_n & \mathbf{0}_{n\times n} & \mathbf{0}_{n\times m} & \mathbf{0}_{n\times n} & -W\mathcal{L}_c \\ \mathbf{0}_{n\times n} & \alpha\mathcal{L}_cW & \mathbf{0}_{n\times m} & \mathbf{0}_{n\times n} & \mathbf{0}_{n\times n} \end{bmatrix},\ B_{cl}(\rho)=\begin{bmatrix} \mathbf{0}_{n\times 1} \\ \mathbf{0}_{n\times 1} \\ \mathbf{0}_{m\times 1} \\ \mathbf{1}_n \\ \mathbf{0}_{n\times 1} \end{bmatrix},$$
$$C_{cl}=\begin{bmatrix} C & \mathbf{0}_{2n\times 2n} \end{bmatrix}. \tag{15}$$

satisfies the following algebraic equations:

$$\mathbf{0}_{n\times 1}=\bar{I}_t-Y\bar{V}-\mathbb{B}_e\bar{I}, \tag{18a}$$
$$\mathbf{0}_{n\times 1}=(K_P-\mathbf{I}_n)\bar{V}-R_t\bar{I}_t+K_I\bar{v}+KW\mathcal{L}_c\bar{x}_c, \tag{18b}$$
$$\mathbf{0}_{m\times 1}=-R\bar{I}+\mathbb{B}_e^T\bar{V}, \tag{18c}$$
$$\mathbf{0}_{n\times 1}=-\bar{V}+V^*\mathbf{1}_n-W\mathcal{L}_c\bar{x}_c, \tag{18d}$$
$$\mathbf{0}_{n\times 1}=\alpha\mathcal{L}_cW\bar{I}_t. \tag{18e}$$

Let Assumption 1 hold and K_I is a non-singular matrix. Using the properties of kernel of $\mathcal{L}_c$ and $\mathbf{1}_n^T\mathbb{B}_e=\mathbf{0}_{1\times m}$, from the above equations, one can obtain that

$$\bar{I}_t=\frac{1}{\mathbf{1}_n^TW^{-1}\mathbf{1}_n}W^{-1}\mathbf{1}_n\mathbf{1}_n^TY\bar{V}, \tag{19a}$$
$$\bar{I}=R^{-1}\mathbb{B}_e^T\bar{V}, \tag{19b}$$
$$\bar{v}=K_I^{-1}\left((\mathbf{I}_n-K_P+K)\bar{V}+R_t\bar{I}_t-K\mathbf{1}_nV^*\right), \tag{19c}$$
$$\bar{x}_c=\frac{1}{n}\mathbf{1}_n\mathbf{1}_n^Tx_c(0)+\mathcal{L}_c^+W^{-1}\left(-\bar{V}+\mathbf{1}_nV^*\right), \tag{19d}$$
$$0=\mathbf{1}_n^TW^{-1}\bar{V}-\mathbf{1}_n^TW^{-1}\mathbf{1}_nV^* \tag{19e}$$

where $\mathcal{L}_c^+$ is the generalized inverse of $\mathcal{L}_c$ and $(\bar{V},\bar{I}_t)$ satisfies the following equations obtained by Kirchoff's law:

$$\bar{I}_t=(Y+\mathbb{B}_eR^{-1}\mathbb{B}_e^T)\bar{V}. \tag{20}$$

From (19a) and (20), we have

$$\frac{1}{\mathbf{1}_n^TW^{-1}\mathbf{1}_n}W^{-1}\mathbf{1}_n\mathbf{1}_n^TY\bar{V}=(Y+\mathbb{B}_eR^{-1}\mathbb{B}_e^T)\bar{V}. \tag{21}$$

Hence, $\bar{V}$ can be obtained by the solution of the following equation:

$$\mathcal{A}_V\bar{V}=\mathcal{B}_V, \tag{22}$$

where

$$\mathcal{A}_V=\begin{bmatrix} \frac{1}{\mathbf{1}_n^TW^{-1}\mathbf{1}_n}W^{-1}\mathbf{1}_n\mathbf{1}_n^TY-(Y+\mathbb{B}_eR^{-1}\mathbb{B}_e^T) \\ \mathbf{1}_n^TW^{-1} \end{bmatrix},$$
$$\mathcal{B}_V=\begin{bmatrix} \mathbf{0}_{n\times 1} \\ \mathbf{1}_n^TW^{-1}\mathbf{1}_nV^* \end{bmatrix}. \tag{23}$$

The solvability of (22) was discussed in [17].

Proposition 1. *Let Assumption 1 hold. The current sharing and voltage balancing in* (9) *and* (10) *are simultaneously achieved at the equilibrium point of the closed-loop system.*

Proof: According to (14) and the dynamics of $x_i^c(t)$ in (12), at equilibrium point $\bar{I}_t$, one has $\mathcal{L}_cW\bar{I}_t=\mathbf{0}_{n\times 1}$. Under Assumption 1, $\mathcal{L}_c$ has a simple zero eigenvalue [18]. Thus, $W\bar{I}_t=I_t^*\mathbf{1}_n$ is the solution of $\mathcal{L}_cW\bar{I}_t=\mathbf{0}_{n\times 1}$, where $I_t^*\in\mathbb{R}$ is the consensus value. Moreover, based on the dynamics of $v_i(t)$ in (11) and the properties of the Laplacian matrix $\mathcal{L}_c$, at equilibrium point $\bar{V}$, one has $\mathbf{1}_n^TW^{-1}\bar{V}=\mathbf{1}_n^TW^{-1}\mathbf{1}_nV^*$.

IV. Stability Analysis

This section analyzes the stability and performance of the DC microgrid with the dynamics given in (14).

Theorem 1. *Consider the closed-loop LPV microgrid system in* (14) *and* (15) *with the scheduling parameters in* (7) *whose rate of variation is given in* (8)*. If the parameters of the PI-based primary control in* (11) *and secondary control in* (12) *belong to the following set:*

$$\mathcal{X}_{[i]}=\left\{\begin{matrix} K_{P_i}<1, \quad 0<K_{I_i}<\dfrac{R_{t_i}}{L_{t_i}}\left(1-K_{P_i}\right), \\ K_i=K_{P_i}-1,\ \alpha>0 \end{matrix}\right\}. \tag{24}$$

for $i=1,\ldots,n$. Then, the equilibrium $\bar{x}_{cl}$ of the LPV model presented by (14) is asymptotically stable.

Proof: We consider the following parameter-dependent Lyapunov function:

$$V_p=(x_{cl}(t)-\bar{x}_{cl})^TP(\rho)(x_{cl}(t)-\bar{x}_{cl}), \tag{25}$$

where

$$P(\rho)=\begin{bmatrix} C_t & \mathbf{0}_{n\times n} & \mathbf{0}_{n\times m} & \mathbf{0}_{n\times n} & \mathbf{0}_{n\times n} \\ \star & -R_t\beta^{-1} & \mathbf{0}_{n\times m} & K_I\beta^{-1} & \mathbf{0}_{n\times n} \\ \star & \star & L & \mathbf{0}_{m\times n} & \mathbf{0}_{m\times n} \\ \star & \star & \star & (K_P-\mathbf{I}_n)K_I\beta^{-1} & \mathbf{0}_{n\times n} \\ \star & \star & \star & \star & \mathbf{I}_n \end{bmatrix} \tag{26}$$

where $\beta=K_I+L_t^{-1}(K_P-\mathbf{I}_n)R_t$. First, we show that $P(\rho)\succ 0$, $\forall\rho\in\Phi$. According to the Schur complement lemma [19], $P(\rho)\succ 0$ if and only if the following conditions are satisfied:

$$\begin{bmatrix} C_t & \mathbf{0}_{n\times n} & \mathbf{0}_{n\times n} \\ \star & -R_t\beta^{-1} & \mathbf{0}_{n\times n} \\ \star & \star & L \end{bmatrix}\succ 0,$$
$$\begin{bmatrix} C_t & \mathbf{0}_{n\times n} & \mathbf{0}_{n\times n} \\ \star & -R_t\beta^{-1}-K_I\beta^{-1}(K_P-\mathbf{I}_n)^{-1}L_t & \mathbf{0}_{n\times n} \\ \star & \star & L \end{bmatrix}\succ 0. \tag{27}$$

By direct calculation, it can be shown that $R_t\beta^{-1}+K_I\beta^{-1}(K_P-\mathbf{I}_n)^{-1}L_t=L_t(K_P-\mathbf{I}_n)^{-1}$. The set of the control parameters in (24) implies that $\beta\prec 0$ and $L_t(K_p-\mathbf{I}_n)^{-1}\prec 0$. As a result, the inequality conditions in (27) are satisfied for $\forall\rho\in\Phi$; hence, $P(\rho)\succ 0$, $\forall\rho\in\Phi$.

According to the Lyapunov theory, the closed-loop microgrid dynamics in (14) is exponentially stable if

$$Q = \underbrace{A_{cl}^T(\rho)P(\rho) + P(\rho)A_{cl}(\rho)}_{Q_P(\rho)} + \underbrace{\sum_{i=1}^{q=3n} \dot{\rho}_i \frac{\partial P(\rho)}{\partial \rho_i}}_{\dot{P}(\rho)} \prec 0,\ \forall \rho \in \Phi, \tag{28}$$

where $\rho_1 = C_t$, $\rho_2 = R_t$, and $\rho_3 = L_t$. By direct calculation, $Q_P(\rho)$ is obtained as follows:

$$Q_p(\rho) = -\begin{bmatrix} 2Y & \mathbf{0}_{n\times m} & \mathbf{0}_{n\times m} & \mathbf{0}_{n\times n} & \mathbf{0}_{n\times n} \\ \star & -2R_t^2\beta^{-1} & \mathbf{0}_{n\times m} & 2R_tK_I\beta^{-1} & \mathbf{0}_{n\times n} \\ \star & \star & 2R & \mathbf{0}_{m\times n} & \mathbf{0}_{m\times n} \\ \star & \star & \star & -2K_I^2\beta^{-1} & \mathbf{0}_{n\times n} \\ \star & \star & \star & \star & \mathbf{0}_{n\times n} \end{bmatrix}. \tag{29}$$

As the following constraints are satisfied, based on the Schur complement lemma, $Q_p(\rho) \preceq 0$, $\forall \rho \in \Phi$.

$$\begin{gathered} -\begin{bmatrix} 2R & \mathbf{0}_{m\times n} & \mathbf{0}_{m\times n} \\ \star & -2K_I^2\beta^{-1} & \mathbf{0}_{n\times n} \\ \star & \star & \mathbf{0}_{n\times n} \end{bmatrix} \preceq 0, \\ -\begin{bmatrix} 2R & \mathbf{0}_{m\times n} & \mathbf{0}_{m\times n} \\ \star & \mathbf{0}_{n\times n} & \mathbf{0}_{n\times n} \\ \star & \star & \mathbf{0}_{n\times n} \end{bmatrix} \preceq 0. \end{gathered} \tag{30}$$

In the next stage, $\dot{P}(\rho)$ is obtained in (32), where $\frac{\partial \beta^{-1}}{\partial R_t} = -\beta^{-1}L_t^{-1}(K_P - \mathbf{I}_n)\beta^{-1}$ and $\frac{\partial \beta^{-1}}{\partial L_t} = \beta^{-1}L_t^{-2}(K_P - \mathbf{I}_n)R_t\beta^{-1}$. Taking into account the set $\mathcal{X}_{[i]}$, it can be shown that $\frac{\partial \beta^{-1}}{\partial R_t}$ is a diagonal matrix with positive diagonal entities while and $\frac{\partial \beta^{-1}}{\partial L_t}$ is a diagonal matrix with negative diagonal entities. By applying the Schur Complement Lemma, it can be shown that $\frac{\partial P(\rho)}{\partial \rho_2} \prec 0$ and $\frac{\partial P(\rho)}{\partial \rho_3} \succ 0$. Taking into account the rate of variation of ρ in (8), one can shown that

$$\dot{\rho}_1 \frac{\partial P(\rho)}{\partial \rho_1} \preceq 0,\ \dot{\rho}_2 \frac{\partial P(\rho)}{\partial \rho_2} \preceq 0,\ \dot{\rho}_3 \frac{\partial P(\rho)}{\partial \rho_3} \preceq 0,\ \forall \rho \in \Phi. \tag{31}$$

Thus, it can be shown that $Q \preceq 0$, $\forall \rho \in \Phi$. We then use the LaSalle's invariance principle to show that the state trajectories of (14) converge to the largest invariant set contained entirely in $\Psi = \{x_{cl} : \dot{V}_p = (x_{cl}(t) - \bar{x}_{cl})^T Q(\rho)(x_{cl}(t) - \bar{x}_{cl}) = 0\}$. It can be shown that the set Ψ only contains $\bar{x}_{cl}$. Hence, $\bar{x}_{cl}$ is asymptotically stable.

Remark 2. *It can be shown that the set of $\mathcal{X}_{[i]}$, for $i = 1, \ldots, n$ is not empty. Furthermore, the integral control gain K_{I_i} should be chosen so that $0 < K_{I_i} < \frac{R_{t_i,nom}}{L_{t_i,nom}}(1 - K_{P_i})$.*

V. Simulation Results and Analysis

In this section, the performance and effectiveness of the reliability-aware secondary control scheme is evaluated by a set of simulation case studies. To this end, we consider a meshed DC microgrid with 6 DG units whose topology is depicted in Fig. 1. The parameters of the DG units and power lines are taken from [20].

In the following, two case studies are conducted to evaluate the performance of the proposed control scheme in voltage balancing and proportional current sharing while under inductance and capacitance uncertainties.

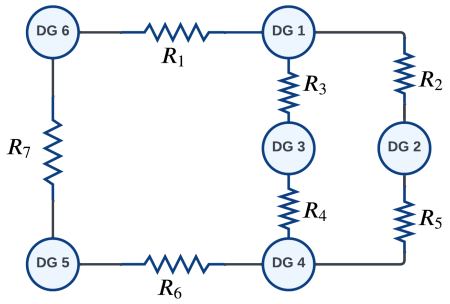

Fig. 1. Schematic diagram of the physical layer of a meshed DC microgrid consisting of $n = 6$ DG units connected by $m = 7$ power lines.

In the first case study, it is assumed that the value of ESR and inductance of the power converter of DG 1 is changed at $t = 3$ s. The inductance value is continuously decreasing from its nominal value to 0.7 of its value while its ESR is increasing from its nominal value to 1.7 of its value. Fig. 2 shows the voltage and current of the power converter (V_i, I_{t_i}), $i = 1, \ldots, 6$, with the proposed secondary control scheme. As one can observe from this figure, upon parameter time-varying changes at $t = 3$ s, the proposed secondary control scheme allows voltage balancing and proportional current sharing amongst all DG units.

In the second case study, the robustness of the proposed distributed secondary control scheme is validated against the time-varying changes in the capacitance value. To this end, it is assumed that the value of the capacitor of DG 5 is changing as follows:

$$C_{t_5}(t) = \begin{cases} C_{t_5,nom} & \text{for } t \leq 3, \\ (1 - 0.1(t-3))C_{t_5,nom} & \text{for } 3 < t < 5, \\ 0.8C_{t_5,nom} & \text{for } t \geq 5 \end{cases} \tag{33}$$

where $C_{t_5,nom}$ is the nominal value of C_{t_5}. The microgrid voltage and current trajectories are shown in Fig. 3.

VI. Conclusions

This paper developed a reliability-aware distributed secondary control scheme for cyber-physical DC microgrids. In the proposed approach, the DC microgrid under the degradation process of power converters' parameters was modeled by a linear parameter varying (LPV) dynamical system. By leveraging tools from the stability analysis of LPV systems, as well as insights from the physics of microgrids, a novel reliability-oriented distributed secondary control scheme was proposed. The DC microgrid with the proposed secondary control scheme guarantees stability and ensures voltage balancing and current sharing while taking the reliability aspects and stability constraints into the control design process. Simulation results demonstrated the performance and effectiveness of the proposed control scheme.

$$\dot{P}(\rho) = \mathrm{diag}(\dot{C}_t, \mathbf{0}_{n\times n}, \mathbf{0}_{m\times m}, \mathbf{0}_{n\times n}, \mathbf{0}_{n\times n}) + \begin{bmatrix} \mathbf{0}_{n\times n} & \mathbf{0}_{n\times n} & \mathbf{0}_{n\times m} & \mathbf{0}_{n\times n} & \mathbf{0}_{n\times n} \\ \star & -R_t\frac{\partial\beta^{-1}}{\partial L_t}\dot{L}_t & \mathbf{0}_{n\times m} & K_I\frac{\partial\beta^{-1}}{\partial L_t}\dot{L}_t & \mathbf{0}_{n\times n} \\ \star & \star & \mathbf{0}_{m\times m} & \mathbf{0}_{m\times n} & \mathbf{0}_{m\times n} \\ \star & \star & \star & (K_P-\mathbf{I}_n)K_I\frac{\partial\beta^{-1}}{\partial L_t}\dot{L}_t & \mathbf{0}_{n\times n} \\ \star & \star & \star & \star & \mathbf{0}_{n\times n} \end{bmatrix} + \begin{bmatrix} \mathbf{0}_{n\times n} & \mathbf{0}_{n\times n} & \mathbf{0}_{n\times m} & \mathbf{0}_{n\times n} & \mathbf{0}_{n\times n} \\ \star & (-\beta^{-1}-R_t\frac{\partial\beta^{-1}}{\partial R_t})\dot{R}_t & \mathbf{0}_{n\times m} & K_I\frac{\partial\beta^{-1}}{\partial R_t}\dot{R}_t & \mathbf{0}_{n\times n} \\ \star & \star & \mathbf{0}_{m\times m} & \mathbf{0}_{m\times n} & \mathbf{0}_{m\times n} \\ \star & \star & \star & (K_P-\mathbf{I}_n)K_I\frac{\partial\beta^{-1}}{\partial R_t}\dot{R}_t & \mathbf{0}_{n\times n} \\ \star & \star & \star & \star & \mathbf{0}_{n\times n} \end{bmatrix}. \tag{32}$$

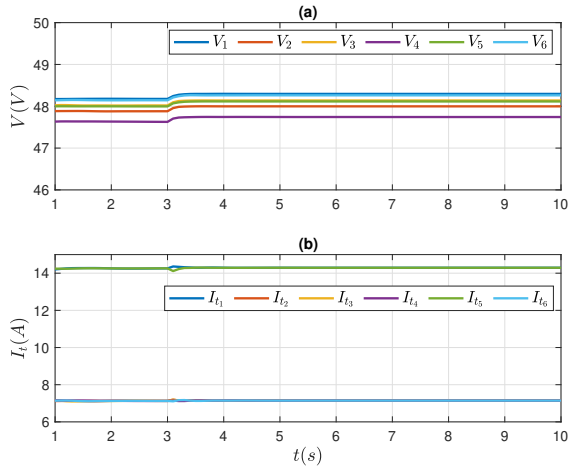

Fig. 2. Voltage and current trajectories of the meshed DC microgrid with the proposed secondary controller in the presence of time-varying changes of the inductance and ESR of the power converter of DG 1.

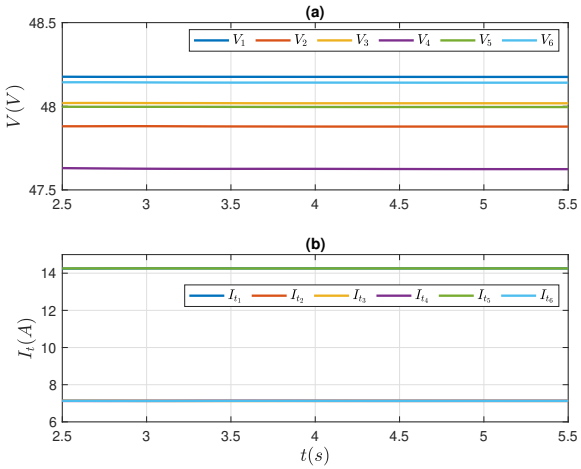

Fig. 3. Voltage and current trajectories of the meshed DC microgrid with the proposed secondary controller in the presence of time-varying changes of the capacitance of power converter of DG 5.

REFERENCES

[1] M. S. Sadabadi, "Privacy-informed consensus-based secondary control in cyber-physical dc microgrids," *IEEE Control Systems Letters*, vol. 7, pp. 2089–2094, 2023.

[2] M. S. Sadabadi, S. Sahoo, and F. Blaabjerg, "Stability-oriented design of cyberattack-resilient controllers for cooperative dc microgrids," *IEEE Transactions on Power Electronics*, vol. 37, no. 2, pp. 1310–1321, 2022.

[3] H. Wang and F. Blaabjerg, "Power electronics reliability: State of the art and outlook," *IEEE Journal of Emerging and Selected Topics in Power Electronics*, vol. 9, no. 6, pp. 6476–6493, 2021.

[4] S. Peyghami, P. Palensky, and F. Blaabjerg, "An overview on the reliability of modern power electronic based power systems," *IEEE Open Journal of Power Electronics*, vol. 1, pp. 34–50, 2020.

[5] N. Dhere, "Reliability of PV modules and balance-of-system components," in *Conference Record of the Thirty-first IEEE Photovoltaic Specialists Conference, 2005.*, 2005, pp. 1570–1576.

[6] Y. Song and B. Wang, "Survey on reliability of power electronic systems," *IEEE Transactions on Power Electronics*, vol. 28, no. 1, pp. 591–604, 2013.

[7] S. Peyghami, P. Davari, and F. Blaabjerg, "System-level reliability-oriented power sharing strategy for dc power systems," *IEEE Transactions on Industry Applications*, vol. 55, no. 5, pp. 4865–4875, 2019.

[8] M. Ghadrdan, B. Abdi, S. Peyghami, H. Mokhtari, and F. Blaabjerg, "On-line condition monitoring system for dc-link capacitor of back-to-back converters using large-signal transients," *IEEE Journal of Emerging and Selected Topics in Power Electronics*, vol. 11, no. 1, pp. 1132–1142, 2023.

[9] Y. Peng, S. Zhao, and H. Wang, "A digital twin based estimation method for health indicators of dc–dc converters," *IEEE Transactions on Power Electronics*, vol. 36, no. 2, pp. 2105–2118, 2021.

[10] M. Ghadrdan, S. Peyghami, H. Mokhtari, and F. Blaabjerg, "Condition monitoring of dc-link electrolytic capacitor in back-to-back converters based on dissipation factor," *IEEE Transactions on Power Electronics*, vol. 37, no. 8, pp. 9733–9744, 2022.

[11] Y. Song, S. Sahoo, Y. Yang, and F. Blaabjerg, "Stability constraints on reliability-oriented control of ac microgrids – theoretical margin and solutions," *IEEE Transactions on Power Electronics*, vol. 38, no. 8, pp. 9459–9468, 2023.

[12] J. Mohammadpour and C. W. Scherer, *Control of linear parameter varying systems with applications*. Springer New York, NY, 2012.

[13] M. S. Sadabadi, "Line-independent plug-and-play voltage stabilization and L_2 gain performance of DC microgrids," *IEEE Control Systems Letters*, vol. 5, no. 5, pp. 1609–1614, Nov. 2021.

[14] Z. Cen and P. Stewart, "Condition parameter estimation for photovoltaic buck converters based on adaptive model observers," *IEEE Transactions on Reliability*, vol. 66, no. 1, pp. 148–160, 2017.

[15] S. Chen, S. Wang, P. Wen, and S. Zhao, "Digital twin for degradation parameters identification of dc-dc converters based on bayesian optimization," in *2021 IEEE International Conference on Prognostics and Health Management (ICPHM)*, 2021, pp. 1–9.

[16] H. Soliman, H. Wang, and F. Blaabjerg, "A review of the condition monitoring of capacitors in power electronic converters," *IEEE Transactions on Industry Applications*, vol. 52, no. 6, pp. 4976–4989, 2016.

[17] M. S. Sadabadi, N. Mijatovic, and T. Dragičević, "A robust cooperative distributed secondary control strategy for dc microgrids with fewer communication requirements," *IEEE Transactions on Power Electronics*, vol. 38, no. 1, pp. 271–282, 2023.

[18] F. Bullo, *Lectures on Network Systems*, 1.6 ed. Kindle Direct Publishing, 2022. [Online]. Available: http://motion.me.ucsb.edu/book-lns

[19] R. A. Horn and C. R. Johnson, *Matrix Analysis*. United States of America: Cambridge University Press, 1990.

[20] M. S. Sadabadi, Q. Shafiee, and A. Karimi, "Plug-and-play robust voltage control of DC microgrids," *IEEE Transactions on Smart Grid*, vol. 9, no. 6, pp. 6886–6896, Nov. 2018.